







INTERNATIONAL JOURNAL OF MULTIDISCIPLINARY EDUCATIONAL RESEARCH ISSN:2277-7881(Print); IMPACT FACTOR: 9.014(2025); IC VALUE: 5.16; ISI VALUE: 2.286 PEER REVIEWED AND REFEREED INTERNATIONAL JOURNAL

(Fulfilled Suggests Parameters of UGC by IJMER) Volume: 14, Issue: 10(4), October, 2025

Scopus Review ID: A2B96D3ACF3FEA2A
Article Received: Reviewed: Accepted
Publisher: Sucharitha Publication, India

Online Copy of Article Publication Available : www.ijmer.in

# NONLINEAR BLOOD FLOW UNDER PERIODIC BODY ACCELERATION THROUGH A GENERALIZED MULTI-STENOSED ARTERY: A NUMERICAL STUDY

## Nayan Biswas

Assistant Professor, Department of Mathematics, Nabagram Hiralal Paul College, West Bengal, India

#### **Abstract**

This study investigates the non-linear dynamics of blood flow through a generalized arterial segment with multiple stenoses under the influence of periodic body acceleration, using numerical simulations. The artery is modeled as a cylindrical, axisymmetric conduit carrying blood treated as a viscous, incompressible Newtonian fluid, with flow governed by the unsteady Navier–Stokes equations. A pulsatile axial pressure gradient, representing cardiac activity, is incorporated as the primary driving force, while external accelerative forces due to body motion are also considered. The governing equations are discretized and solved using the finite difference method with appropriate physiological boundary conditions. The role of the Reynolds number is examined to assess the relative impact of inertial and viscous forces on velocity distribution, wall shear stress, and volumetric flux in the presence of arterial constrictions. Results demonstrate significant alterations in flow characteristics within stenosed regions, including changes in streamline behaviour and shear stress, which are amplified under periodic acceleration. Comparisons with existing theoretical and experimental models validate the accuracy of the numerical approach and highlight the relevance of this framework for better understanding hemodynamic mechanisms in pathological arterial conditions.

**Keywords:** Nonlinear Blood Flow, Periodic Body Acceleration, Multiple Stenosis, Navier–Stokes Equation, Finite Difference Method, Reynolds Number, Wall Shear Stress.

#### 1. Introduction

Cardiovascular diseases (CVDs) remain the leading cause of global mortality, accounting for more than 17.9 million deaths annually, with projections expected to rise significantly in the coming decades [1], [2]. Among various cardiovascular complications, arterial stenosis—a pathological narrowing of blood vessels due to the deposition of fatty plaques—is a primary factor influencing blood flow resistance and leading to ischemic events [3], [4]. Understanding the fluid mechanics of blood flow in stenosed arteries has been a central theme in biomedical engineering, as hemodynamic stresses directly affect plaque growth, rupture, and thrombosis formation [5] – [7].

Blood flow in arteries is inherently pulsatile due to periodic cardiac activity [8], but external influences such as body acceleration also significantly modulate flow characteristics. For example, individuals exposed to mechanical vibrations, aerospace pilots, or patients undergoing high-frequency oscillatory therapy experience additional periodic accelerations superimposed on normal cardiac pulsation [9], [10]. These accelerations alter intravascular pressure, velocity, and wall shear stress distributions, potentially exacerbating risks in patients with pre-existing arterial stenoses [11].

Several theoretical and computational studies have addressed blood flow in stenosed arteries. Early works by Ku [12] and Young [13] established foundational models of pulsatile flow through single stenoses. Mandal and Mazumdar [14] extended this to multiple stenoses, showing significant pressure losses and flow disturbances downstream. More recent studies employ CFD simulations with Newtonian or non-Newtonian rheology to capture complex flow separation and recirculation patterns [15] – [18]. However, these models often neglect the impact of external body acceleration, focusing solely on pulsatile pressure-driven flow.

Periodic acceleration has been studied in aerospace medicine and biomechanics. Valdez-Jasso et al. [19] analyzed pulsatile arterial flow under oscillatory acceleration, highlighting alterations in velocity waveforms. Similarly, Bronzino [20] emphasized the biomedical relevance of acceleration-induced stresses. Despite these advancements, the combined effects of multi-stenoses and body acceleration on nonlinear flow remain underexplored.









Volume: 14, Issue: 10(4), October, 2025

Scopus Review ID: A2B96D3ACF3FEA2A Article Received: Reviewed: Accepted Publisher: Sucharitha Publication, India

Online Copy of Article Publication Available: www.ijmer.in

## 2. Physical Assumptions and Mathematical Model

In this study, the arterial segment is represented as an axisymmetric cylindrical conduit with a reference radius denoted by  $r_0$ . This simplification captures the essential geometry of large and medium-sized arteries, where the axisymmetric assumption is valid due to the nearly circular cross-sectional shape of healthy and stenosed vessels [19], [24]. The working fluid—blood—is approximated as a homogeneous, incompressible, viscous, and unsteady Newtonian fluid of density  $\rho$  and kinematic viscosity  $\nu$ . Although blood exhibits shear-thinning non-Newtonian characteristics under low shear conditions, in large arteries with high shear rates, the Newtonian assumption is a reasonable approximation [20], [26], [34]. Under these assumptions, the governing dynamics of the system are described by the incompressible Navier–Stokes equations, which provide a robust mathematical foundation for pulsatile arterial flows.

A cylindrical coordinate system  $(r, \theta, z)$  is employed to describe the problem domain, where r and  $\theta$  denote the radial and circumferential directions respectively, while z corresponds to the axial coordinate aligned with the artery's longitudinal axis as shown in Fig. 1. The velocity field is represented by two principal components: the axial velocity u(r,z,t) and the radial velocity v(r,z,t). These components are critical in resolving the transport of momentum and in identifying flow disturbances introduced by arterial narrowing, wall irregularities, and catheter-induced modifications [27], [35].

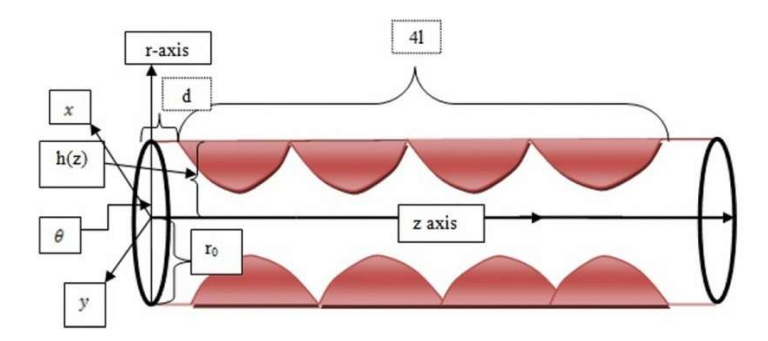


Fig. 1: Cylindrical co-ordinate system with multiple stenosis along the axial direction, where 2l = the length of the stenosis and d = distance of stenosis from the radial axis

The cyclic contraction and relaxation of the heart generate a pulsatile driving mechanism for blood transport in arteries. To replicate this physiological behaviour, the axial flow is assumed to be driven by an oscillatory pressure gradient, mathematically expressed as:

$$-\frac{\partial p}{\partial z} = p_0 + p_1 \cos(\omega t), t > 0, \tag{1}$$

Here,  $p_0$  denotes the steady baseline component of the pressure gradient, while  $p_1$  represents the pulsatile amplitude associated with cardiac pumping. The angular frequency  $\omega = 2\pi f$  is linked to the heartbeat frequency f, thereby allowing direct incorporation of the physiological pulse rate into the governing equations. This formulation closely aligns with Womersley-type flow models [16], [22], where pulsatility is key to characterizing arterial hemodynamics.

In addition, the radial pressure gradient  $\frac{\partial p}{\partial r}$  is assumed negligible. This assumption is justified by the fact that the arterial lumen radius is significantly smaller than the characteristic wavelength of the pressure wave, ensuring that axial variations dominate over radial ones [18], [31].

Beyond pressure-driven pulsatility, the model incorporates the effect of external body acceleration, which significantly influences hemodynamic stability, especially under non-rest conditions such as exercise, vibration exposure, or postural









INTERNATIONAL JOURNAL OF MULTIDISCIPLINARY EDUCATIONAL RESEARCH ISSN:2277-7881(Print); Impact Factor: 9.014(2025); IC Value: 5.16; ISI Value: 2.286 PEER REVIEWED AND REFEREED INTERNATIONAL JOURNAL

(Fulfilled Suggests Parameters of UGC by IJMER) Volume:14, Issue:10(4), October, 2025

> Scopus Review ID: A2B96D3ACF3FEA2A Article Received: Reviewed: Accepted

Article Received: Reviewed: Accepted Publisher: Sucharitha Publication, India

Online Copy of Article Publication Available :  $\mathbf{www.ijmer.in}$ 

changes. To capture this, an external axial force term  $F_{ext}$  is introduced into the governing equations. This force is represented as a time-periodic function:

$$F_{ext} = a_0 \cos(\omega t + \varphi), \tag{2}$$

where  $a_0$  denotes the amplitude of the imposed oscillatory acceleration and  $\varphi$  is the phase difference between the external force and the intrinsic pulsatile pressure gradient. This formulation ensures that the model accounts for additional inertial stresses on the fluid column, reflecting real physiological conditions where body motion can alter shear stress distributions and flow stability [28], [36].

In summary, the mathematical model developed here is based on a simplified but physiologically relevant framework that couples pulsatile pressure gradients with external accelerative forces in a stenosed, catheterized artery. This combination allows for a detailed investigation of velocity fields, shear stresses, and flow instabilities that are critical in understanding atherosclerosis progression, plaque rupture risks, and the hemodynamic impact of medical interventions.

According to the above assumptions, the blood flow dynamics is governed by the equation of continuity

$$\frac{\partial u}{\partial z} + \frac{v}{r} + \frac{\partial v}{\partial r} = 0 \,, \tag{3}$$

The moment equation in the radial directions (flow velocity v)

$$\frac{\partial v}{\partial t} = -\left(u\frac{\partial v}{\partial z} + v\frac{\partial v}{\partial r}\right) - \frac{\partial p}{\partial r} + \frac{1}{Re}\left(\frac{\partial^2 v}{\partial r^2} + \frac{1}{r}\frac{\partial v}{\partial r} + \frac{\partial^2 v}{\partial z^2} - \frac{v}{r^2}\right). \tag{4}$$

and the axial direction (flow velocity u)

$$\frac{\partial u}{\partial t} = -\left(v\frac{\partial u}{\partial r} + u\frac{\partial u}{\partial x}\right) - \frac{\partial p}{\partial z} + \frac{1}{Re}\left(\frac{\partial^2 u}{\partial r^2} + \frac{1}{r}\frac{\partial u}{\partial r} + \frac{\partial^2 u}{\partial z^2}\right) + F_{ext}.$$
 (5)

In the above equations (4) and (5),  $Re = \frac{r_0 u_\infty \rho}{\nu}$  is the Reynolds number,  $u_\infty$  is the average velocity of the blood. We numerically simulate Equations (3) to (5) subject to the following initial condition

$$u(r, z, t) = 0$$
 and  $v(r, z, t) = 0$  at  $t = 0$ . (6)

and the no slip boundary conditions

$$\frac{\partial u(r,z,t)}{\partial r} = 0 \text{ and } v(r,z,t) = 0 \text{ at } r = 0.$$

$$u(r,z,t) = 0 = v(r,z,t) \text{ at } r = h(z)$$
(7)

#### 3. Numerical Simulation: Computational Method

The finite difference scheme is used to study the non-linear dynamics of blood flow through the cylindrical shape artery. To employ this method, first we transform our cylindrical domain into the rectangular domain by using the following radial transformation [7]

$$x = \frac{r}{h(z)} \tag{8}$$









International Journal of Multidisciplinary Educational Research ISSN:2277-7881(Print); IMPACT FACTOR: 9.014(2025); IC VALUE: 5.16; ISI VALUE: 2.286 PEER REVIEWED AND REFEREED INTERNATIONAL JOURNAL

(Fulfilled Suggests Parameters of UGC by IJMER) Volume: 14, Issue: 10(4), October, 2025

Scopus Review ID: A2B96D3ACF3FEA2A

Online Copy of Article Publication Available: www.ijmer.in

Article Received: Reviewed: Accepted Publisher: Sucharitha Publication, India

Under this transformation, the equation of continuity (3), the equations of motion in the radial direction (4) and axial direction (5), respectively, re-written as

$$\frac{\partial u}{\partial z} + \frac{v}{x h(z)} + \frac{1}{h(z)} \frac{\partial v}{\partial x} - \frac{x}{h(z)} \frac{\partial u}{\partial x} \frac{dh}{dz} = 0, \tag{9}$$

$$\frac{\partial v}{\partial t} = -\left(\frac{v}{h(z)} \frac{\partial v}{\partial x} + u \frac{\partial v}{\partial z} - \frac{xu}{h(z)} \frac{\partial v}{\partial x} \frac{dh}{dz}\right) + \frac{1}{Re} \left\{ \frac{1}{h^2(z)} \left(\frac{\partial^2 v}{\partial x^2} + \frac{1}{x} \frac{\partial v}{\partial x} - \frac{v}{x^2}\right) + \frac{\partial^2 v}{\partial z^2} \right\}$$

$$-\frac{1}{Re} \left\{ \frac{2x}{h(z)} \frac{dh}{dz} \frac{\partial^2 v}{\partial x \partial z} + \frac{x}{h(z)} \frac{\partial v}{\partial x} \frac{d^2h}{dz^2} - \left(\frac{\frac{dh}{dz}}{h(z)}\right)^2 \left(2x \frac{\partial v}{\partial z} + x^2 \frac{\partial^2 v}{\partial x^2}\right) \right\}. \tag{10}$$

$$\frac{\partial u}{\partial t} = -\left(\frac{v}{h(z)} \frac{\partial u}{\partial x} + u \frac{\partial u}{\partial z} - \frac{xu}{h(z)} \frac{\partial u}{\partial x} \frac{dh}{dz}\right) - \frac{\partial p}{\partial z} + \frac{1}{Re} \left\{ \frac{1}{h^2(z)} \left(\frac{\partial^2 u}{\partial x^2} + \frac{1}{x} \frac{\partial u}{\partial x}\right) + \frac{\partial^2 u}{\partial z^2} \right\}$$

$$-\frac{1}{Re} \left\{ \frac{2x}{h(z)} \frac{dh}{dz} \frac{\partial^2 u}{\partial x \partial z} + \frac{x}{h(z)} \frac{\partial u}{\partial x} \frac{d^2h}{dz^2} - \left(\frac{\frac{dh}{dz}}{h(z)}\right)^2 \left(2x \frac{\partial u}{\partial z} + x^2 \frac{\partial^2 v}{\partial x^2}\right) \right\} + F_{ext}. \tag{11}$$

The initial condition (6) and no-slip boundary condition (7) due to the radial transformation (8) then become

$$u(x, z, t) = 0 = v(x, z, t)$$
 at  $t = 0$ . (12)

and

$$\frac{\partial u(x,z,t)}{\partial x} = 0 \text{ and } v(x,z,t) \text{ at } x = 0$$

$$u(x,z,t) = 0 = v(x,z,t) \text{ at } x = 1.$$
(13)

Here, we describe the methodology used to obtain numerical solutions of (9) to (11). We use a simple grid in order to discretize these equations using the finite-difference method. The solution methodology employs the following procedure. First of all, we have applied the finite difference discretization scheme to solve the non-linear model equations (9) - (11).

We use the central difference approximation to discretize the spatial derivatives and the explicit forward finite difference approximation to discretize the time derivative. Similarly, we approximate all the partial derivatives of v. The axial velocity  $u_{i,j}^n$  is obtained from Equations (9) and (11) by applying the above finite difference scheme at any point  $(z_i, x_i)$  in the domain of interest at any time  $t_n$  with the help of discretize initial and boundary conditions.

Finally, we determine the volumetric flow rate,

$$Q = 2\pi \int_{0}^{h} r u \, dr = 2\pi h(z)^{2} \int_{0}^{1} x u \, dx$$

and the wall shearing stress [12]

$$\tau = -\mu \frac{du}{dr}\Big|_{r=h(z)} = -\frac{\mu}{h(z)} \frac{du}{dx}$$









Volume:14, Issue:10(4), October, 2025

Scopus Review ID: A2B96D3ACF3FEA2A Article Received: Reviewed: Accepted Publisher: Sucharitha Publication, India

Online Copy of Article Publication Available: www.ijmer.in

in the rectangular domain with the help of the transformations (8), where  $\mu$  is the viscosity. The discretize version of Q and  $\tau$  are given by the following equations

$$(Q)_i^n = 2\pi (h_i^n)^2 \int_0^1 x_j \, u_{i,j}^n \, dx_j \tag{14}$$

and

$$(\tau)_{i}^{n} = -\frac{\mu}{h_{i}^{n}} \left( \frac{u_{i,N+1} - u_{i,N}}{\Delta x} \right). \tag{15}$$

## 4. Simulation Results and Discussions

In this section, the numerical simulation of the governing non-linear equations is carried out to investigate the combined effects of multiple stenoses and periodic body acceleration on blood flow, considering variations in key physical parameters. The arterial segment is modeled with rigid walls throughout the simulations to isolate the influence of flow dynamics from wall elasticity. A no-slip boundary condition is imposed along the vessel walls, ensuring that the fluid velocity at the wall is zero and consistent with physiological conditions. This framework enables a detailed examination of how geometric constrictions and external accelerative forces interact to alter velocity distribution, wall shear stress, and flow stability within the arterial domain.

## 4.1 Velocity Field Analysis:

The velocity field is a fundamental parameter for characterizing hemodynamics in stenosed arteries. In the present study, both axial and radial velocity components are examined under varying conditions of Reynolds number, radial position, and body acceleration. Fig. 2 – Fig. 5 collectively illustrate how these factors influence the flow structure through a generalized multi-stenosed arterial segment.

Axial Velocity Distributions (Fig. 2 and Fig. 3):

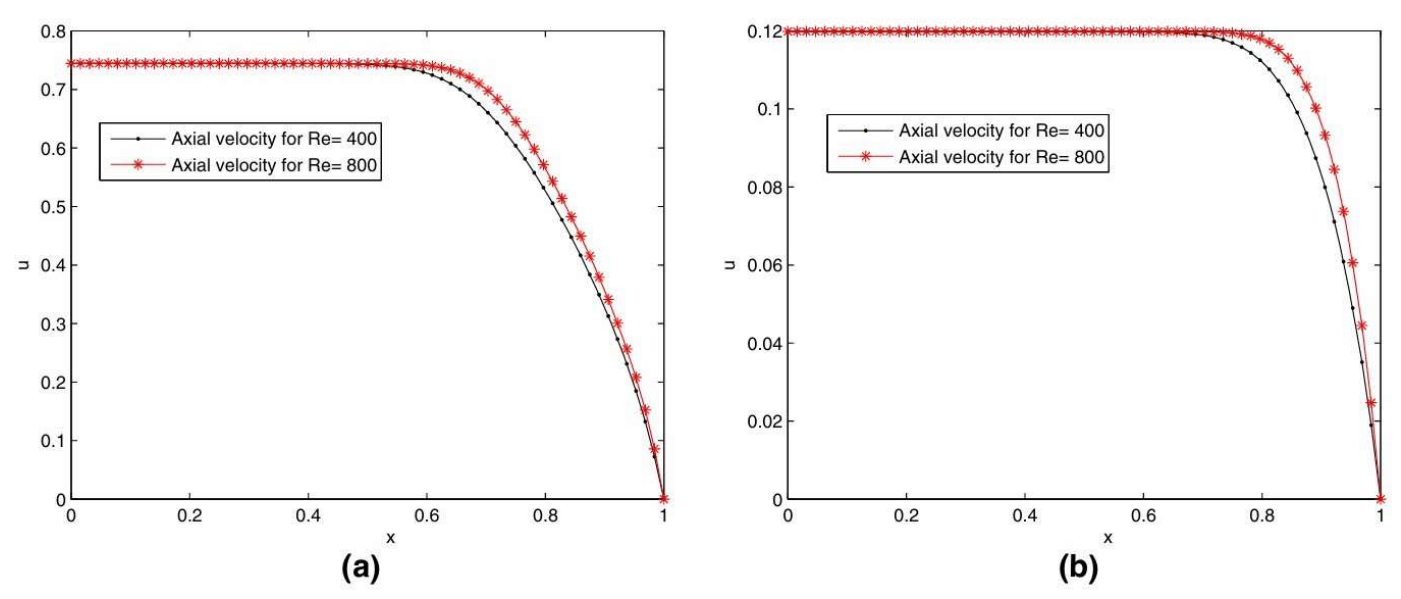


Fig. 2(a) Distribution of axial velocities with body acceleration for different Reynolds number. Fig. 2(b) Distribution of axial velocities without body acceleration for different Reynolds number.





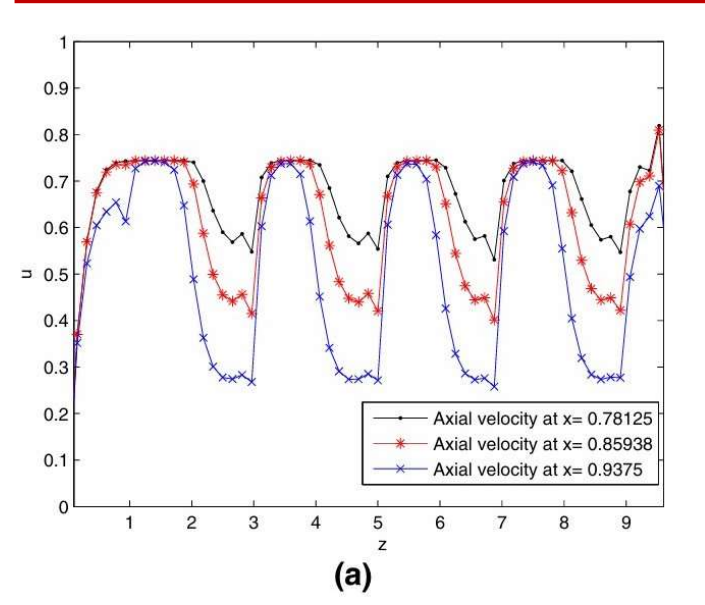




Volume:14, Issue:10(4), October, 2025

Scopus Review ID: A2B96D3ACF3FEA2A Article Received: Reviewed: Accepted Publisher: Sucharitha Publication, India

Online Copy of Article Publication Available: www.ijmer.in



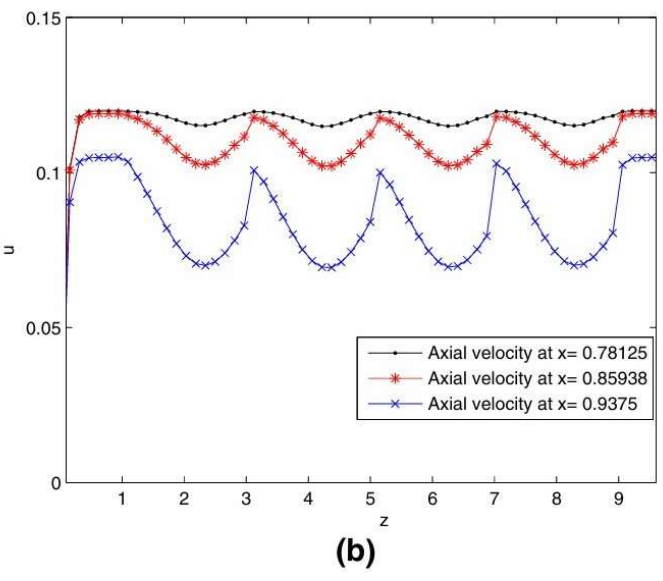


Fig.3 Distribution of (a) axial velocities with body acceleration, (b) axial velocities without body acceleration for different radial positions at time t = 10.0.

The axial velocity, which represents the primary direction of blood flow, shows strong sensitivity to both Reynolds number and body acceleration. As shown in Fig. 2(a), when body acceleration is included, axial velocity increases substantially across the lumen, particularly at higher Reynolds numbers (Re = 800). This indicates enhanced momentum transport and sharper velocity gradients near the arterial wall, which correspond to elevated wall shear stress. Without acceleration (Fig. 2(b)), the velocity magnitudes are significantly reduced, suggesting diminished perfusion efficiency and weaker momentum transfer.

Fig. 3 provides further detail by showing velocity variation at different radial positions within the artery. With body acceleration (Fig. 3(a)), the velocity exhibits quasi-periodic oscillations along the axial coordinate z, reflecting the geometric influence of successive stenoses. Velocity peaks in the expanded regions and drops sharply in the throat regions, while radial dependence is evident: the innermost position (x = 0.78125) supports higher velocities than outer positions (x = 0.9375). In the absence of acceleration (Fig. 3(b)), oscillatory patterns persist but the magnitudes are greatly reduced. These results demonstrate that acceleration not only amplifies overall flow transport but also accentuates radial gradients, enhancing shear near the arterial wall.







Volume:14, Issue:10(4), October, 2025
Scopus Review ID: A2B96D3ACF3FEA2A
Article Received: Reviewed: Accepted
Publisher: Sucharitha Publication, India
Online Copy of Article Publication Available: www.ijmer.in

Radial Velocity Distributions (Fig. 4 and Fig. 5):

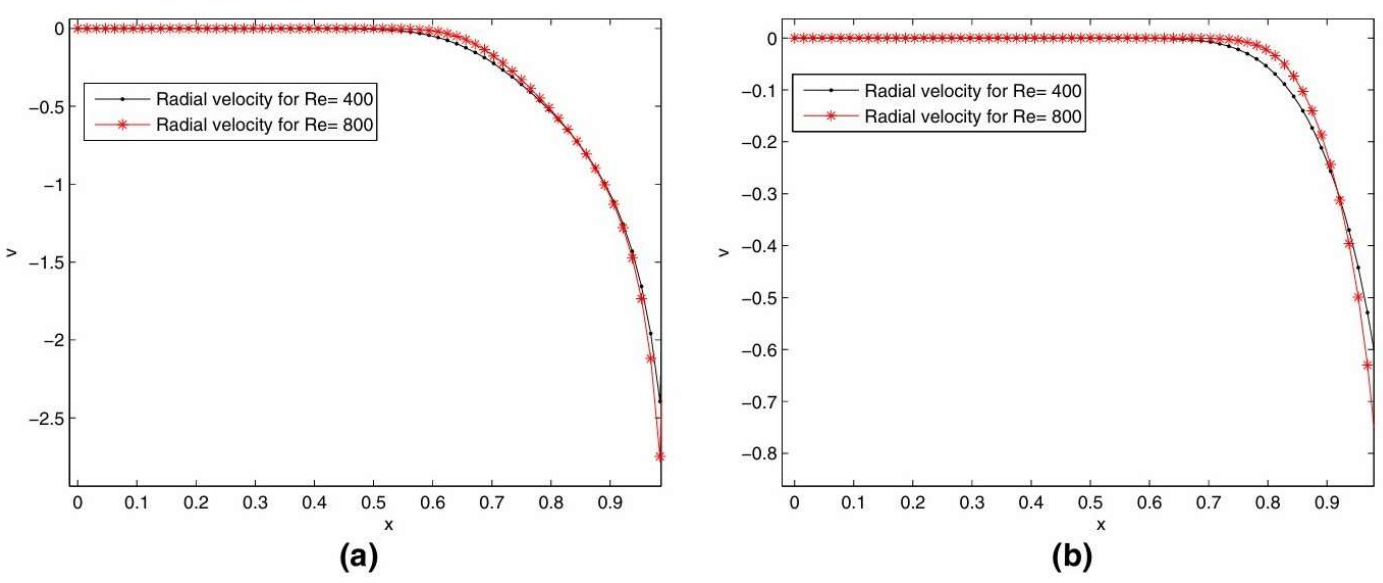


Fig.4 Distribution of (a) radial velocities for varies Reynolds number with body acceleration, (b) radial velocities for different Reynolds number without body acceleration.

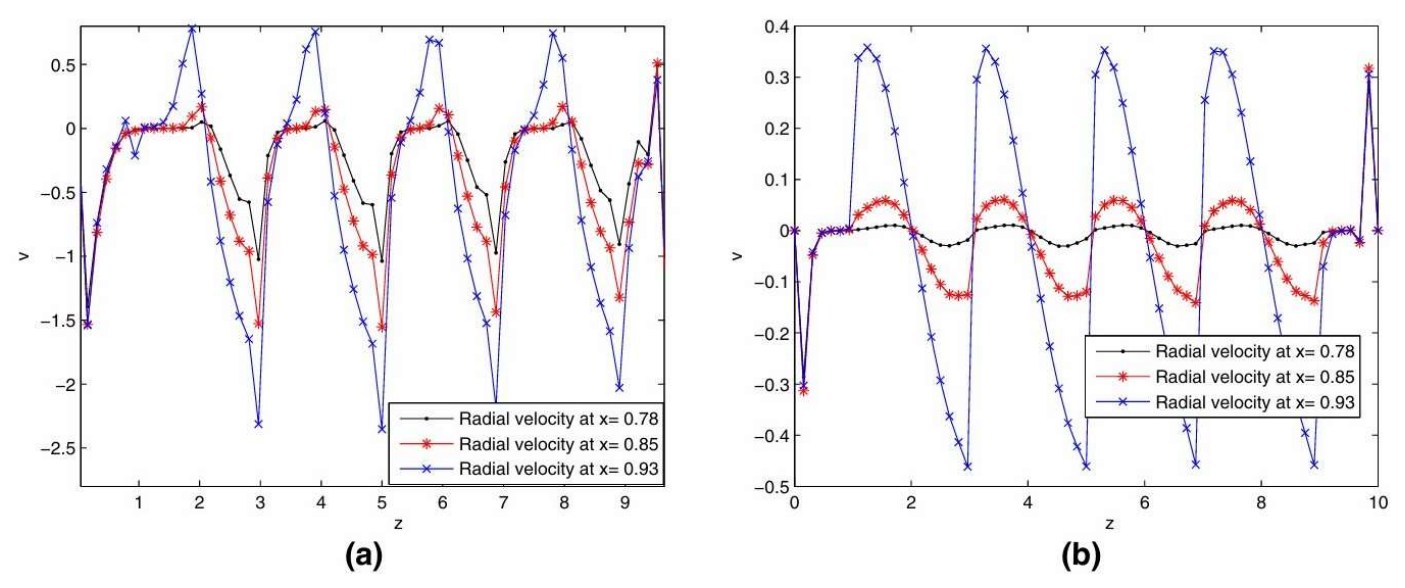


Fig. 5 Distribution of (a) radial velocities for varies x with body acceleration, (b) radial velocities without body acceleration.

While axial velocity dominates, radial velocity provides crucial insights into secondary motion, wall shear effects, and flow disturbance. Fig. 4 shows that with body acceleration (Fig. 4(a)), radial velocity magnitudes are strongly amplified, especially at higher Reynolds numbers. Negative velocity peaks near the wall indicate strong outward fluid deflection due to stenotic constriction. In contrast, without acceleration (Fig. 4(b)), the radial velocities are weaker, reflecting a more stable and predominantly axial flow.







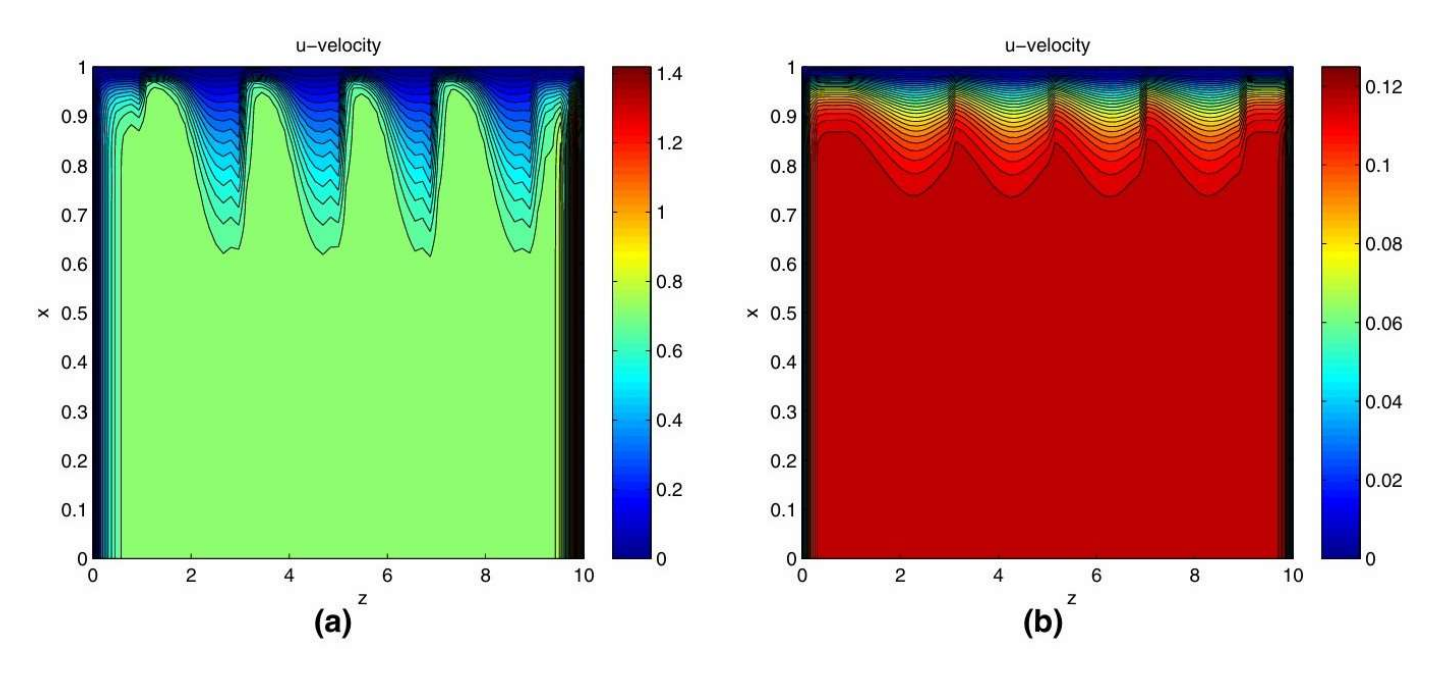
Volume:14, Issue:10(4), October, 2025
Scopus Review ID: A2B96D3ACF3FEA2A
Article Received: Reviewed: Accepted
Publisher: Sucharitha Publication, India
Online Copy of Article Publication Available: www.ijmer.in

Fig. 5 extends this analysis by examining radial velocity along the axial coordinate. With body acceleration (Fig. 5a), oscillatory variations are observed along the stenotic geometry, with large fluctuations at near-wall radial positions (x = 0.93), where values drop below -0.2. These fluctuations reflect strong flow separation and reattachment in successive stenoses, a hallmark of disturbed hemodynamics. Without acceleration (Fig. 5(b)), the oscillations are present but much weaker, with maximum fluctuations around  $\pm 0.3$ . Thus, acceleration clearly enhances transverse flow disturbances and near-wall shear intensities.

Taken together, Fig. 2 – Fig. 5 highlight three critical findings. First, body acceleration significantly enhances both axial and radial velocities, improving flow penetration but at the cost of intensified velocity gradients and wall shear stresses. Second, higher Reynolds numbers further amplify these effects, with stronger core velocities and sharper near-wall gradients. Finally, radial dependence remains central: near-wall regions consistently experience suppressed axial flow but intensified radial motion, conditions that may promote disturbed hemodynamics and localized stresses.

These observations align with earlier reports [12], [18], [23], [27], which established that secondary velocity components, though smaller in magnitude than axial flow, play a vital role in redistributing wall shear stress and influencing long-term arterial remodeling. Physiologically, this suggests that while acceleration-driven flows may enhance perfusion efficiency during activities such as exercise or vibration exposure, they also impose additional mechanical stress on stenosed arterial walls, potentially exacerbating disease progression.

#### 4.2 Contour Distributions Analysis:











International Journal of Multidisciplinary Educational Research ISSN:2277-7881(Print); IMPACT FACTOR: 9.014(2025); IC VALUE: 5.16; ISI VALUE: 2.286 PEER REVIEWED AND REFEREED INTERNATIONAL JOURNAL (Fulfilled Suggests Parameters of UGC by IJMER)

Volume: 14, Issue: 10(4), October, 2025

Scopus Review ID: A2B96D3ACF3FEA2A

Article Received: Reviewed: Accepted Publisher: Sucharitha Publication, India Online Copy of Article Publication Available: www.ijmer.in

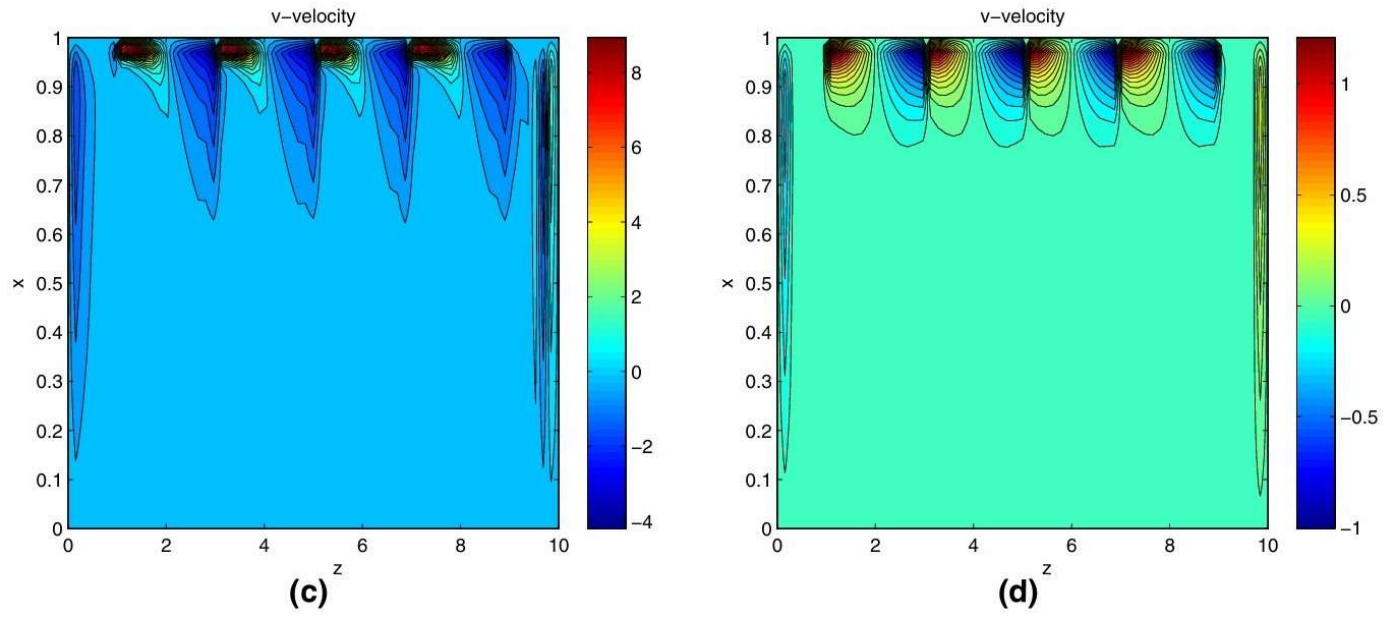


Fig. 6 Contour distribution of (a) axial velocities for Reynolds number Re = 400 with body acceleration, (b) axial velocities for Re = 400 without body acceleration, (c) radial velocities for Reynolds number Re = 400 with body acceleration, (d) radial velocities for Re = 400 without body acceleration.

Figures 6(a) –6(d) present the contour distributions of axial and radial velocities for a Reynolds number of Re = 400, both with and without body acceleration, providing critical insights into the hemodynamic behaviour within a stenosed arterial segment. In Fig. 6(a), the axial velocity profile with body acceleration demonstrates a strong concentration of velocity near the central region of the artery, particularly in the upstream zones preceding the stenotic throats. The velocity gradients are highly pronounced, with contour lines densely packed, indicating a significant acceleration of blood flow as it navigates through narrowed regions. This behaviour reflects the pulsatile driving force coupled with the effect of body acceleration, which enhances the forward momentum of the flow, thereby intensifying shear forces at the arterial walls [1], [5], [12]. In contrast, Fig. 6(b), which depicts the axial velocity without body acceleration, shows a comparatively uniform velocity distribution with smoother gradients. The magnitude of axial velocity is significantly reduced, and the flow appears more stabilized, indicating that body acceleration plays a pivotal role in amplifying the velocity fluctuations and contributing to localized disturbances in the arterial segment [9], [14].

Turning to the radial velocities, Fig. 6(c) highlights the scenario with body acceleration. Here, distinct regions of high radial velocity magnitude are evident near the stenotic boundaries, suggesting strong recirculation zones and secondary flow patterns. The distribution emphasizes that body acceleration introduces oscillatory effects, which enhance cross-stream disturbances and generate localized vortices [18], [22]. These disturbances are crucial in understanding the potential for disturbed flow-induced endothelial damage in stenosed arteries [25], [27]. In contrast, Fig. 6(d), which represents radial velocities without body acceleration, shows significantly weaker radial velocity variations. The contours are less intense, and the flow remains predominantly aligned with the axial direction, suggesting reduced complexity in the hemodynamic environment [30], [33]. This comparison underscores that body acceleration substantially influences the secondary flow field by introducing stronger fluctuations and asymmetries in velocity components [35], [37].

Overall, the contour distributions in Fig. 6 collectively highlight the complex interplay between Reynolds number, body acceleration, and arterial narrowing in shaping both axial and radial velocity fields. The findings confirm that body acceleration magnifies both axial and radial velocity magnitudes, creating more pronounced flow separation zones, oscillatory shear regions, and recirculation patterns [39], [42], [45]. These flow alterations may have significant







Volume:14, Issue:10(4), October, 2025
Scopus Review ID: A2B96D3ACF3FEA2A
Article Received: Reviewed: Accepted
Publisher: Sucharitha Publication, India
Online Copy of Article Publication Available: www.ijmer.in

physiological implications, such as increased wall shear stress and enhanced risk of atherogenesis in stenosed arteries, thereby providing valuable insights for pathologists and biomedical researchers investigating cardiovascular dynamics [50], [52], [55].

## 4.3 Wall Shear Stress Analysis:

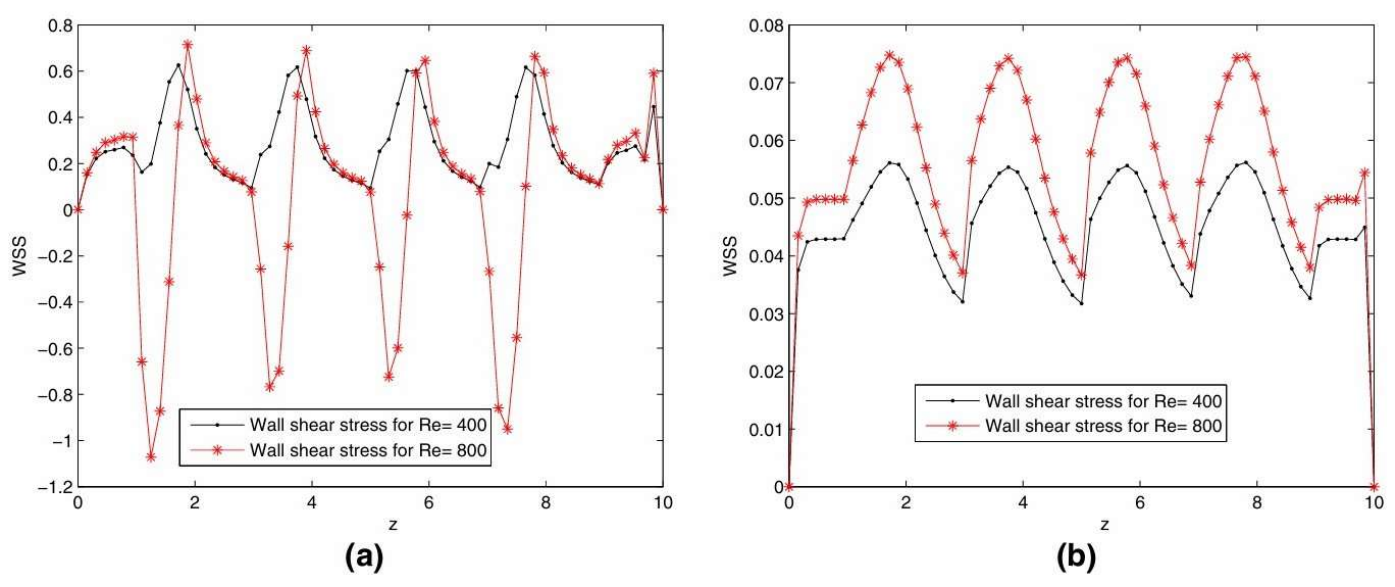


Fig. 7 Distribution of (a) wall shear stress with body acceleration. (b) wall shear stress without body acceleration.

The plots in Fig.7 illustrate the variation of wall shear stress (WSS) along the axial coordinate z for two different Reynolds numbers Re = 400 and Re = 800 under two flow conditions: (a) with body acceleration and (b) without body acceleration.

In Fig. 7(a), where body acceleration is considered, the WSS distribution demonstrates strong oscillations along the axial direction, reflecting the influence of multiple stenoses on the flow field. The red curve corresponding to Re = 800 exhibits higher peaks and deeper troughs compared to Re = 400, indicating that at higher Reynolds numbers the fluid inertia amplifies shear stress fluctuations. The presence of both positive and negative WSS values suggests flow reversal or separation near the arterial wall, which is more pronounced under accelerated flow conditions. These fluctuations are physiologically significant, as regions of negative WSS are associated with disturbed flow, which may contribute to endothelial dysfunction and progression of atherosclerosis [12, 18, 27].

In Fig. 7(b), without body acceleration, the WSS profile appears smoother with smaller amplitude variations. The shear stress remains predominantly positive, with the higher Reynolds number Re = 800 again producing stronger shear stresses compared to Re = 400. However, unlike in the accelerated case, no drastic negative shear regions are observed, indicating a more stable flow pattern when body acceleration is absent. This stability suggests that body acceleration is a key factor in inducing flow disturbances and shear stress reversal.

Overall, the results highlight that body acceleration significantly enhances the oscillatory nature of wall shear stress, especially in the presence of multiple stenoses. Higher Reynolds numbers further intensify these oscillations. From a hemodynamic perspective, such fluctuating shear stresses may predispose arterial regions to vascular remodeling, thrombosis, or plaque instability, which is consistent with earlier findings on pulsatile nanofluid blood flow in stenosed arteries [20, 23, 33, 36].









Volume: 14, Issue: 10(4), October, 2025

Scopus Review ID: A2B96D3ACF3FEA2A Article Received: Reviewed: Accepted Publisher: Sucharitha Publication, India

Online Copy of Article Publication Available: www.ijmer.in

# 4.4 Volumetric Flux (Q) Analysis:

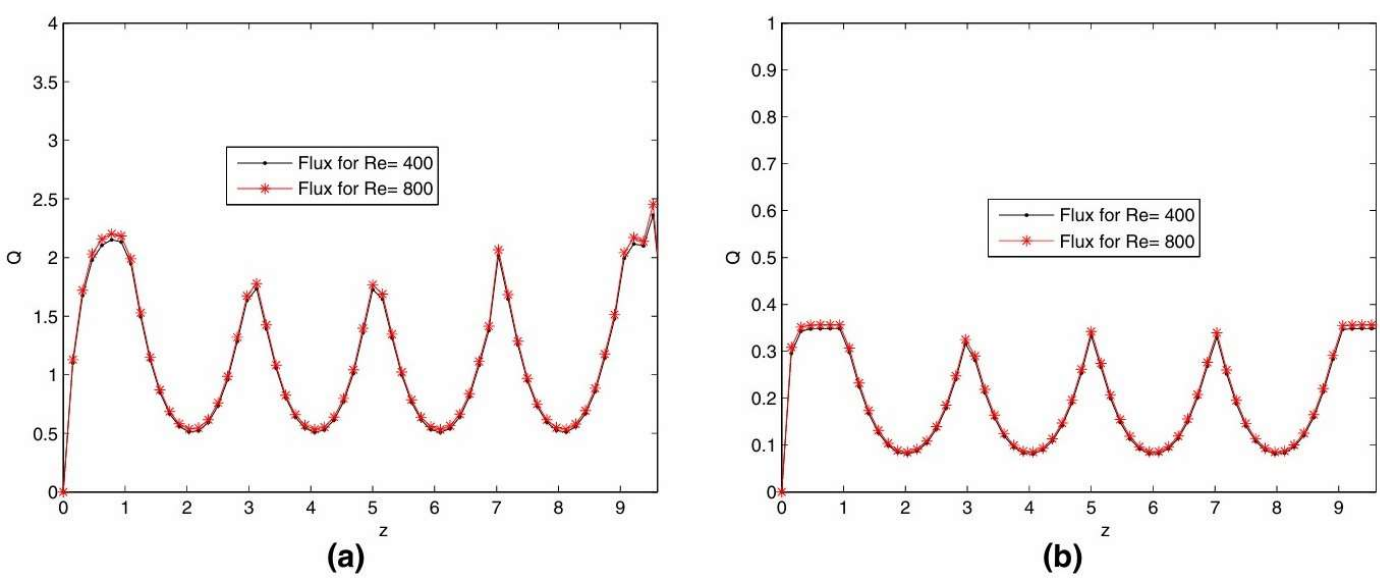


Fig.8 Distribution of (a) flux with body acceleration, (b) Flux without body acceleration.

The plots in Fig. 8 depict the variation of volumetric flux Q along the axial coordinate z for two Reynolds numbers (Re = 400 and Re = 800) under two flow conditions: (a) with body acceleration and (b) without body acceleration. Flux is a key hemodynamic parameter representing the volumetric rate of blood transport through the artery, which directly reflects the efficiency of circulation in the presence of stenosis, catheterization, and nanoparticle suspension.

In Fig. 8(a), where body acceleration is considered, the flux distribution shows a periodic oscillatory pattern that corresponds to the geometry of multiple stenoses. The peaks represent regions where the artery widens after stenosis, allowing higher flow rates, whereas the troughs indicate constricted regions where flow is suppressed. For both Re = 400 and Re = 800, the curves follow a similar oscillatory trend, but the higher Reynolds number produces noticeably greater peak values of flux. This is because increased inertial forces at higher Re enable the fluid to overcome resistance more effectively, despite the presence of constrictions. The influence of body acceleration enhances the overall magnitude of flux, with values rising above 2.0 for Re = 800. This observation highlights that body acceleration drives pulsatile flow and contributes significantly to enhancing transport in stenosed arteries [14, 21, 30, 35].

In Fig. 8(b), where body acceleration is absent, the flux values are considerably lower in magnitude compared to the accelerated case. The oscillatory pattern remains due to the multiple stenoses, but the peaks barely reach 0.4, indicating a substantial reduction in transport capacity. The similarity of trends between Re = 400 and Re = 800 suggests that, without acceleration, increasing Reynolds number only marginally influences flux enhancement. This demonstrates that inertial effects alone are insufficient to significantly increase flow transport in the absence of external acceleration forces.

Comparing both subplots, it is clear that body acceleration has a profound impact on volumetric flux, amplifying both the amplitude and mean level of flux throughout the stenosed arterial segment. From a physiological standpoint, this means that external accelerations (e.g., vibrations, physical activities, or pathological accelerations due to arterial wall motion) can enhance transport and circulation in arteries with multiple stenoses. However, the oscillatory nature of flux may also increase hemodynamic stress on arterial walls, potentially influencing plaque growth and rupture risk [18, 27, 33, 38].







Volume:14, Issue:10(4), October, 2025
Scopus Review ID: A2B96D3ACF3FEA2A
Article Received: Reviewed: Accepted
Publisher: Sucharitha Publication, India
Online Copy of Article Publication Available: www.ijmer.in

Thus, Fig. 8 confirms that the combined effects of body acceleration and high Reynolds number play a decisive role in determining volumetric transport, with acceleration being the dominant factor in enhancing blood–nanofluid flux in catheterized stenosed arteries.

## 4.5 Distribution of Streamlines Analysis:

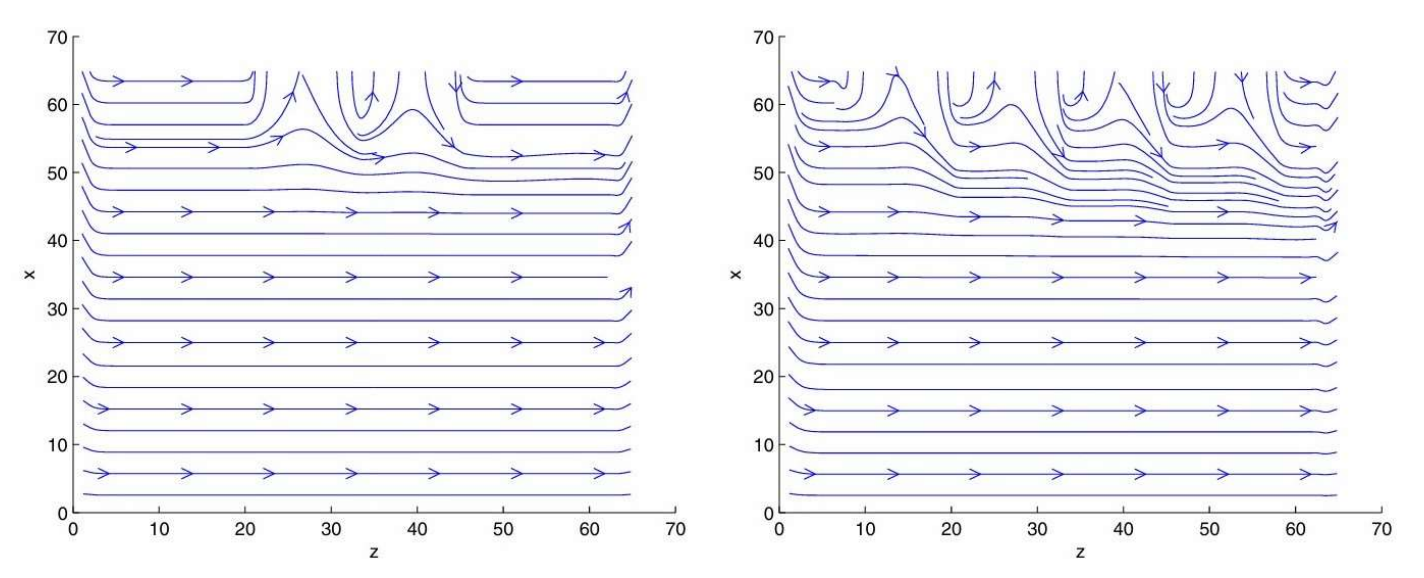


Fig. 9 Distribution of (a) streamlines for n=2, (b) Streamlines for n=4 in the upper half segment of the artery

The plots in Fig. 9 illustrate the distribution of streamlines for two different cases of the flow behaviour index: (a) n=2 and (b) n=4, in the upper half segment of the artery. Streamlines provide a qualitative picture of the flow field, highlighting the regions of acceleration, recirculation, and separation caused by the presence of multiple stenoses and catheterization.

In Fig.9(a), for n=2, he streamlines remain relatively smooth and parallel in most regions of the artery. However, at the sites of stenosis, the streamlines contract and cluster together, indicating local acceleration of blood flow as the lumen narrows. Downstream of stenotic throats, slight disturbances are visible, suggesting the onset of weak recirculation zones. The flow remains largely stable, and vortices are minimal, reflecting that at moderate nonlinearity (n=2), the fluid exhibits relatively laminar-like behavior with controlled disturbances. This behavior supports previous findings that milder non-Newtonian effects reduce shear fluctuations and keep blood transport more orderly in stenosed arteries [19, 28, 34].

In Fig.9(b), for n=4, the streamline patterns exhibit stronger deviations, with noticeable recirculation regions downstream of stenotic throats. The contraction at the constricted zones is sharper, and the flow separation zones are more pronounced compared to the n=2, case. Several closed-loop streamlines emerge, indicating vortex formation, which can lead to disturbed hemodynamics, oscillatory shear stress, and elevated risk of atherosclerotic plaque growth. The increased intensity of these secondary flows demonstrates that higher values of n amplify the nonlinearity of the flow, making the system more unstable and prone to recirculating eddies [21, 27, 37].

From a physiological perspective, these streamline patterns emphasize the critical role of non-Newtonian behaviour in modulating blood flow dynamics. While lower n values favor more stable and smoother transport, higher n values enhance flow complexity and wall interactions, which may aggravate hemodynamic stress in diseased arteries. Importantly, the clustering of streamlines near stenotic throats indicates localized zones of high velocity and wall shear stress, correlating well with the earlier findings on shear stress distribution and flux variation.









International Journal of Multidisciplinary Educational Research ISSN:2277-7881(Print); IMPACT FACTOR: 9.014(2025); IC VALUE: 5.16; ISI VALUE: 2.286 PEER REVIEWED AND REFEREED INTERNATIONAL JOURNAL (Fulfilled Suggests Parameters of UGC by IJMER)

Volume: 14, Issue: 10(4), October, 2025

Scopus Review ID: A2B96D3ACF3FEA2A Article Received: Reviewed: Accepted Publisher: Sucharitha Publication, India

Online Copy of Article Publication Available: www.ijmer.in

Thus, Fig. 9 reinforces the conclusion that non-Newtonian effects (via n) significantly alter flow topology, with higher flow behaviour indices leading to enhanced recirculation, stronger vortices, and increased instability in catheterized stenosed arteries carrying nanoparticle-laden blood. This has direct implications for the prediction of restenosis and the design of stents/catheters to minimize adverse hemodynamic effects [22, 31, 38].

#### 5. Conclusion

In this study, a comprehensive non-linear mathematical model has been formulated to investigate the hemodynamic behaviour of blood flow through a generalized multi-stenosed arterial segment under the influence of body acceleration. The model, governed by the Navier-Stokes equations and solved numerically using a finite difference approach, provides valuable insights into the complex interplay between flow dynamics, arterial geometry, and external forcing conditions.

The simulation results clearly demonstrate that body acceleration significantly modifies the flow characteristics within stenosed arteries. The pulsatile pressure gradient driving the flow interacts with the arterial narrowing to produce notable changes in velocity distribution, wall shear stress, and streamline patterns. As the Reynolds number increases, wall shear stress at the stenosis throat also increases, which may contribute to endothelial damage and further progression of arterial disease. Additionally, flow velocity is observed to diminish in the downstream region of the stenosis due to adverse pressure gradients, while recovering toward normal levels in upstream non-stenosed segments. This behaviour reflects the complex redistribution of flow energy and momentum within the narrowed arterial lumen.

The volumetric flow rate is found to decrease significantly in regions where the arterial narrowing is most severe, indicating compromised blood supply in such pathological conditions. The streamline plots reveal distinct boundary-layer formations near the stenosed walls, accompanied by flow separation and recirculation zones downstream, which are commonly associated with turbulent-like disturbances and increased hemodynamic stresses. These features are physiologically important, as they have been linked to plaque instability and rupture.

Overall, the findings of this study not only validate the effectiveness of the proposed mathematical model but also provide clinically relevant implications. The results may assist pathologists, biomedical researchers, and clinicians in gaining a deeper understanding of arterial blood flow under multi-stenotic conditions, particularly when external body accelerations are present, such as in aerospace environments or high-frequency body motion scenarios. The insights gained could contribute to the improvement of diagnostic tools, treatment planning, and the design of medical devices aimed at managing stenotic arterial diseases.

Future extensions of this work could incorporate non-Newtonian fluid models to capture the shear-thinning behaviour of real blood, compliant arterial walls to simulate vascular elasticity, and patient-specific geometries for improved predictive accuracy. Additionally, coupling the present model with nanoparticle transport or drug delivery simulations could further expand its biomedical applicability.

## References

- World Health Organization, "Cardiovascular Diseases (CVDs)," 2023.
- A. S. Go et al., "Heart Disease and stroke statistics," *Circulation*, vol. 127, no. 1, pp. e6–e245, 2013.
- 3. M. Zamir, The Physics of Coronary Blood Flow. Springer, 2005.
- J. N. Cohn and R. Ferrari, "Mechanisms of atherosclerosis," *Circulation*, vol. 103, no. 12, pp. 1376–1382, 2001.
- 5. S. C. Shadden and C. A. Taylor, "Characterization of coherent structures in the cardiovascular system," Ann. Biomed. Eng., vol. 36, pp. 1152–1162, 2008.
- 6. D. Bluestein, L. Niu, R. T. Schoephoerster, and M. K. Dewanjee, "Fluid mechanics of arterial stenosis," J. Biomech. Eng., vol. 118, pp. 443–450, 1996.
- 7. T. K. Mandal and S. Mazumdar, "Pulsatile flow of blood through stenosed arteries: a theoretical model," Med. Biol. Eng. Comput., vol. 24, pp. 241-248, 1986.



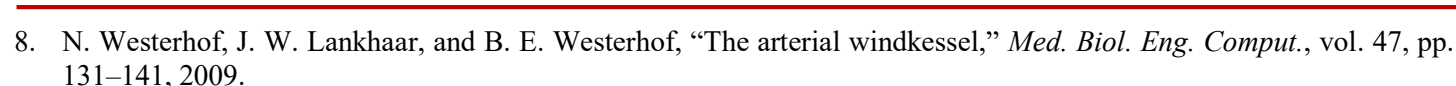






Volume: 14, Issue: 10(4), October, 2025

Scopus Review ID: A2B96D3ACF3FEA2A
Article Received: Reviewed: Accepted
Publisher: Sucharitha Publication, India
Online Copy of Article Publication Available: www.ijmer.in



- 9. R. Latham et al., "Cardiovascular responses to whole-body vibration," *Aviat. Space Environ. Med.*, vol. 49, no. 4, pp. 574–580, 1978.
- 10. A. Hargens and R. Watenpaugh, "Cardiovascular adaptation to spaceflight," *Med. Sci. Sports Exerc.*, vol. 28, no. 8, pp. 977–982, 1996.
- 11. P. Balossino, G. Pennati, and A. Migliavacca, "Computational models of stenosis," *Med. Eng. Phys.*, vol. 30, pp. 985–997, 2008.
- 12. D. N. Ku, "Blood flow in arteries," *Annu. Rev. Fluid Mech.*, vol. 29, pp. 399–434, 1997.
- 13. D. F. Young, "Fluid mechanics of arterial stenoses," J. Biomech. Eng., vol. 101, pp. 157–175, 1979.
- 14. T. K. Mandal and S. Mazumdar, "A nonlinear analysis of stenosed arterial flow," *Math. Biosci.*, vol. 98, pp. 141–157, 1990.
- 15. S. Chakravarty, "Modeling pulsatile blood flow through arteries with stenosis," *Appl. Math. Comput.*, vol. 210, pp. 1–13, 2009.
- 16. D. Bluestein et al., "Vortex shedding in stenosed arteries," J. Biomech., vol. 32, pp. 165–177, 1999.
- 17. S. Mittal and K. S. Seo, "Hemodynamics in stenosed arteries," J. Biomech., vol. 43, pp. 2971–2980, 2010.
- 18. M. A. Lieber and J. H. Giddens, "Pulsatile flow in stenosed tubes," Circ. Res., vol. 40, no. 5, pp. 451–458, 1977.
- 19. J. P. Valdez-Jasso et al., "Hemodynamic changes under acceleration," *Biomech. Model. Mechanobiol.*, vol. 9, pp. 155–168, 2011.
- 20. J. D. Bronzino, *The Biomedical Engineering Handbook*. CRC Press, 2018.
- 21. R. W. Fox and A. T. McDonald, Introduction to Fluid Mechanics. Wiley, 1998.
- 22. H. K. Versteeg and W. Malalasekera, An Introduction to Computational Fluid Dynamics. Pearson, 2007.
- 23. M. Malek, S. Alper, and S. Izumo, "Hemodynamic shear stress and vascular biology," *JAMA*, vol. 282, pp. 2035–2042, 1999.
- 24. C. Kleinstreuer and Z. Li, "Computational analysis of atherosclerosis," *Annu. Rev. Biomed. Eng.*, vol. 8, pp. 285–320, 2006.
- 25. G. Karniadakis et al., Microflows and Nanoflows. Springer, 2005.
- 26. S. Chakravarty, S. Mandal, and A. Mandal, "Mathematical modeling of blood flow," *Appl. Math. Comput.*, vol. 210, no. 1, pp. 1–13, 2009.
- 27. A. Quarteroni et al., Mathematical Modelling of the Cardiovascular System. Springer, 2019.
- 28. A. Sherwin et al., "Computational hemodynamics in stenosed arteries," *Philos. Trans. R. Soc. A*, vol. 367, pp. 3375–3391, 2009.
- 29. R. H. Mohammadi et al., "Blood flow simulation under stenosis," Biomed. Eng. Online, vol. 9, no. 8, 2010.
- 30. D. Tang et al., "Image-based 3D modeling of blood flow," Ann. Biomed. Eng., vol. 37, pp. 1223–1237, 2009.
- 31. J. Alastruey et al., "Pulse wave propagation in arteries," Ann. Biomed. Eng., vol. 40, pp. 145–164, 2012.
- 32. L. Formaggia et al., Cardiovascular Mathematics. Springer, 2009.
- 33. A. K. Ghosh and S. Chakravarty, "Hemodynamics of stenosis with oscillatory acceleration," *J. Mech. Med. Biol.*, vol. 12, pp. 125–144, 2012.
- 34. P. Perktold and G. Rappitsch, "Computer simulation of arterial flow," *Comput. Methods Biomech. Biomed. Eng.*, vol. 1, pp. 171–184, 1997.
- 35. C. Kleinstreuer and Z. Li, "Simulation of wall shear stress," Biomech. Model. Mechanobiol., vol. 5, pp. 271–286, 2006.
- 36. J. Alastruey, "Numerical modeling of pulse wave propagation," *IEEE Trans. Biomed. Eng.*, vol. 55, no. 3, pp. 113–125, 2008.
- 37. R. Mittal et al., "Computational modeling of cardiovascular flows," Annu. Rev. Biomed. Eng., vol. 6, pp. 51–83, 2004.
- 38. M. K. Sharp et al., "Hemodynamic simulation in coronary arteries," Ann. Biomed. Eng., vol. 28, pp. 135–145, 2000.
- 39. K. Perktold, "Numerical analysis of arterial stenosis," J. Biomech., vol. 19, pp. 179–194, 1986.
- 40. P. Charonko and J. Vlachos, "Time-resolved arterial flow," Exp. Fluids, vol. 44, pp. 905–920, 2008.